Dental Materials 40 (2024) 1677–1684

Contents lists available at ScienceDirect

Dental Materials

journal homepage: www.elsevier.com/locate/dental

Full length article

Comparative analysis of optical and numerical models for reflectance and color prediction of monolithic dental resin composites with varying thicknesses☆

Maria Tejada-Casado [a,*], Vincent Duveiller [b], Razvan Ghinea [a,c], Arthur Gautheron [b,d], Raphaël Clerc [b], Jean-Pierre Salomon [e,f,g], María del Mar Pérez [a], Mathieu Hébert [b], Luis Javier Herrera [h]

[a] Department of Optics, Faculty of Science, University of Granada, Campus de Fuentenueva, s/n 18071 Granada, Spain
[b] Université Jean Monnet Saint-Etienne, CNRS, Institut d Optique Graduate School, Laboratoire Hubert Curien UMR 5516, Saint-Étienne, France
[c] Department of Physics, Faculty of Sciences, University of Craiova, 13 AI Cuza Street, Craiova, 200585, Romania
[d] Univ Lyon, INSA-Lyon, Université Claude Bernard Lyon 1, UJM-Saint Etienne, CNRS, Inserm, CREATIS UMR 5220, U1294, Lyon, France
[e] Faculté d'Odontologie de Nancy (CHRU), France
[f] Dental Materials and Prosthodontics Department, Araraquara's Dental School (UNESP, Brazil), Brazil
[g] OHSU, Dental Biomaterials Department, Portland, OR, USA
[h] Department of Computer Architecture and Computer Technology, E.T.S.I.I.T. University of Granada, s/n 18071, Granada, Spain

ARTICLE INFO

Keywords:
Reflectance prediction
Color prediction
Optical models
Four-flux
Kubelka–Munk
Numerical models
Principal component analysis

ABSTRACT

Objective: To assess the prediction accuracy of recent optical and numerical models for the spectral reflectance and color of monolithic samples of dental materials with different thicknesses.

Methods: Samples of dental resin composites of Aura Easy Flow (Ae1, Ae3 and Ae4 shades) and Estelite Universal Flow Super Low (A1, A2, A3, A3.5, A4 and A5 shades) with thicknesses between 0.3 and 1.8 mm, as well as Estelite Universal Flow Medium (A2, A3, OA2 and OA3 shades) with thicknesses between 0.4 and 2.0 mm, were used. Spectral reflectance and transmittance factors of all samples were measured using a X-Rite Color i7 spectrophotometer. Four analytical optical models (2 two-flux models and 2 four-flux models) and two numerical models (PCA-based and L*a*b*-based) were implemented to predict spectral reflectance of all samples and then convert them into CIE-L*a*b* color coordinates (D65 illuminant, 2° Observer). The CIEDE2000 total color difference formula (ΔE_{00}) between predicted and measured colors, and the corresponding 50:50% acceptability and perceptibility thresholds (AT_{00} and PT_{00}) were used for performance assessment.

Results: The best performing optical model was the four-flux model RTE-4F-RT, with an average ΔE_{00} = 0.72 over all samples, 94.87% of the differences below AT_{00} and 65.38% below PT_{00}. The best performing numerical model was L*a*b*-PCHIP (interpolation mode), with an average ΔE_{00} = 0.48, and 100% and 79.69% of the differences below AT_{00} and PT_{00}, respectively.

Significance: Both optical and numerical models offer comparable color prediction accuracy, offering flexibility in model choice. These results help guide decision-making on prediction methods by clarifying their strengths and limitations.

☆ This work has been funded in part by the Grant PID2022.142151OB.I00 funded by MICIU/AEI/10.13039/501100011033 and by the Grant PID2021-128317OB-I00 funded by MCIN/AEI/10.13039/501100011033 and by "ERDF A way of making Europe"; in part by a public grant from the French National Research Agency (ANR) under the "France 2030" investment plan, which has the reference EUR MANUTECH SLEIGHT—ANR-17-EURE-0026; in part by the Université de Lyon, France through program LABEX PRIMES under Grant ANR-11-LABX-0063 within the program Investissements d'Avenir under Grant ANR-11-IDEX-0007, operated by the French National Research Agency and in part by France Life Imaging under Grant ANR-11-INBS-0006 within the program Infrastructures d'Avenir en Biologie Santé, operated by the French National Research Agency.

* Corresponding author.
E-mail addresses: mariatejadac@ugr.es (M. Tejada-Casado), duveiller.vincent@gmail.com (V. Duveiller), rghinea@ugr.es (R. Ghinea), arthur.Gautheron@creatis.insa-lyon.fr (A. Gautheron), raphael.clerc@institutoptique.fr (R. Clerc), jpsalomon61@gmail.com (J.-P. Salomon), mmperez@ugr.es (M.M. Pérez), mathieu.hebert@institutoptique.fr (M. Hébert), jherrera@ugr.es (L.J. Herrera).

https://doi.org/10.1016/j.dental.2024.07.013
Received 7 June 2024; Received in revised form 2 July 2024; Accepted 23 July 2024
Available online 3 August 2024

1. Introduction

When patients undergo dental treatments, they may have specific expectations regarding the final outcome, especially in terms of color and aesthetic rendering. For the practitioner, meeting these expectations and obtaining satisfying results is crucial to ensure patient satisfaction. Thanks to the latest scientific and technological progress in the dental field, restorations can now closely mimic the natural color and translucency of teeth [1–4], and achieve a similar aspect to the surrounding natural dental tissues. Considering the large number of materials and colors available today on the marketplace, selection of the most appropriate material for a given clinical situation may be difficult [5–7]. Dentists must have a keen eye for color and use empirical techniques to achieve precise shade matching between the restoration and the tissues [8].

Currently, color matching is based on the concept of tooth shade, i.e. the colors of the natural teeth and samples from a shade guide are compared by the dental practitioner [9], most often by naked eye and under the lighting of his/her office, calibrated or not. Sometimes, color evaluation may also be supported instrumentally, by using a colorimeter, spectrophotometer, intraoral scanner or a computer vision system [10–14], whose respective pros and cons [15–19] leave room for improvement.

Decision support for dental materials remains a scientific challenge for several reasons. Firstly, color is not a physical quantity that can be measured directly: it is a sensation, produced in the brain after a complex perceptual process which depends on many parameters. Fortunately, color science has established a correlation between perceived colors and measured physical quantities related to light, and the CIE proposed some standard models and procedures to assess color through optical measurement in some simple cases as for instance a planar, uniform, opaque object placed in a uniform, achromatic scene [20]. These procedures can apply to flat slices of dental materials, despite the fact that these slices are rarely opaque. Second part of the challenge is determining the appropriate optical measurement for color assessment in the specific case of dental materials. The standard procedures stand for opaque, strongly scattering media, such as paper for example. However, dental materials are usually very translucent and, therefore, light propagates more deeply into the matter and can keep some directionality. This can lead to artifacts in the measurements (for example a halo around the illuminated area, corresponding to light that escape from detection, a phenomenon called edge loss), which make difficult the analysis of the measured signal, and therefore the color assessment. The last part of the challenge is that light propagation into dental materials, thereby the material aspect, depends on many parameters related with the matter itself (intrinsic optical parameters such as absorption and scattering coefficients, refractive index, depending on the wavelength of visible light), the shape of the material (structural parameters such has the layer thickness, and the lighting (spectral power distribution, angular distribution, etc.). In this context, even though color is the "quantity" that finally we want to assess, spectral methods are the most suitable, where the physical quantities measured are described as a function of the wavelength of light: they enable assessing the color of a sample under any spectral power distribution of the lighting. This is an advantage knowing that an individual may meet a broad variety of lightings in his everyday life. The methods discussed in this paper are primarily spectral, with the exception of one method that directly deals with color coordinates. In addition, our study focuses on the influence on color of a structural parameter: the thickness of the material layer, known to be determinant in the color of dental material samples [2,4,21–23]. In particular, the methods we use seek to perform some physical measurements on one or more samples of a given thickness (calibration samples), and to predict the color of samples of any other thicknesses (test samples).

For that purpose, two main approaches are possible. The first approach, that qualified as "optical approach" consists in (1) describing that light-matter interaction with an optical model, (2) using that model to extract the optical parameters of the considered material from the physical measurements done on the calibration samples, by taking into account the characteristics of the light, the detector, and the sample thickness, and (3) use the model again with the optical parameters previously obtained but with the new layer thicknesses. In this approach, the optical measurements must be consistent with the models, so that the measured values can be correctly interpreted in terms of light propagation.

The second approach – the "numerical approach" – consists in doing measurements with a given device on a set of samples, and interpolating or extrapolating the measured data for other thicknesses. In this approach, in contrast to the optical approach, the physical measurements must allow for correct interpretation in terms of color, in accordance with the recommendations laid down by the CIE.

The two approaches have been followed in other industrial domains, as for example in printing [24]. In the case of dental materials, the issue has been tackled more recently, but studies based on both approaches have also been proposed [25,26] and have shown their effectiveness in predicting accurately the colors of various materials across different thicknesses.

For the present study, among the optical models available, the Kubelka–Munk Reflectance Theory was selected [27–29], which was used to characterize dental materials [30–35] or predict their spectral reflectance factor [36–38]. Despite its simplistic assumptions, it remains the gold standard analytical method for optical characterization of dental materials. Recently, more advanced optical models, based on the four-flux model generalized by Maheu et al. [39], were developed and applied to dental materials to predict their spectral reflectance factors, showing increased prediction accuracy compared to the previous optical models [40]. Regarding the numerical models, two methods relying on regression techniques differing in the data handled for the prediction and the outcome obtained were selected. The first one is based on a Principal Components Analysis (PCA) approach from reflectance values, allowing to estimate both reflectance and color of a new sample [26], while the second method utilizes CIE-L*a*b* color coordinates, and was specifically designed for CIE-L*a*b* color estimations [41].

The comparative study that is proposed rely on the same set of samples, measured with an optical instrument that satisfy the expectations of both approaches: it allows interpretation in terms of light propagation with optical models, and it is designed for color characterization and is therefore compatible with the numerical approach.

Therefore, the objective of this work is to conduct a comparative analysis of the different methods for color prediction in dentistry present in the current literature, evaluating the strengths and limitations of each approach, in terms of ergonomy, time computation, exportability, and other practical considerations. The research hypothesis studied was that optical models and numerical models can provide similar prediction accuracy.

2. Materials and methods

2.1. Specimen preparation

Samples of dental resin composites of different brands and shades were prepared (Table 1). These dental resin composites have been successfully used in aesthetic dentistry for many years [42,43].

For each shade of the Aura Easy Flow and Estelite Universal Flow SuperLow materials, six samples of different thickness (0.3 mm, 0.6 mm, 0.9 mm, 1.2 mm, 1.5 mm, and 1.8 mm), were prepared. For each shade of the Estelite Universal Flow Medium material, eight samples with thickness 0.4 mm, 0.5 mm, 0.8 mm, 1.0 mm, 1.2 mm, 1.5 mm, 1.6 mm and 2.0 mm were fabricated. The flowable dental resin was injected between two glass-slides, whose spacing was controlled with high precision wedges (Mitutoyo company) defining the nominal thickness

Table 1
Names and manufacturers, classification, composition, shade and batch numbers of resin composites (information given by the manufacturers).

Names (Manufacturers)	Classification	Composition	Shade (Batch numbers)
Aura Easy Flow (SDI Ltd.)	Nano-hybrid resin composite	56% inorganic fillers (0.2–1 micron) multifunctional methacrylic esters (UDMA, TEGDMA, Bis-EMA), initiators, stabilizers, pigments.	Ae1 (1906100) Ae3 (190964) Ae4 (190794)
Estelite Universal Flow SuperLow (Tokuyama)	Supra-nano filled resin composite	Spherical silica-zirconia filler (mean particle size: 200 nm), Composite filler Bis-GMA, Bis-MPEPP, TEGDMA, UDMA, Mequinol, Dibutyl hydroxyl toluene, UV absorber.	A1 (10621) A2 (01713) A3 (2178) A3.5 (4064) A4 (5042) A5 (60311)
Estelite Universal Flow Medium (Tokuyama)	Supra-nano filled resin composite	Spherical silica-zirconia filler (mean particle size: 200 nm), Composite filler Bis-GMA, Bis-MPEPP, TEGDMA, UDMA, Mequinol, Dibutyl hydroxyl toluene, UV absorber.	A2 (0717) A3 (2942) OA2 (7122) OA3 (8096)

of the sample. The samples were light-cured with a LED light curing unit (Radii Xpert, SDI) operating at 1500 mW/cm2, according to the curing scheme described in ISO/TR 4049:2009 [44]: each sample was irradiated five times, 40 s each irradiation, at 12-3-6-9 o'clock positions and ending in the center of the sample. The sample diameter, determined by the volume of material deposited, was ranging from 20 mm to 22 mm. The thickness of each sample after curing was tested with a precision micrometer. Although the measured thicknesses were considered in the experiments, samples will be referred to by their nominal thickness hereinafter for clarity.

2.2. Spectral measurements

The spectral measurements (400 nm to 750 nm with 10 nm steps) were performed with a Color i7 spectrophotometer (X-Rite, Grand Rapids, Michigan, USA), and the average of seven successive measurements was considered. The spectrophotometer allows two reflectance modes: (1) the specular included mode (SCI, CIE di:8° geometry [20]), which allows measurement of the total reflectance factor $R_{tot}(\lambda)$ in the terminology of the four-flux model; (2) the specular excluded mode (SCE, CIE de:8°), allowing measurement of the diffuse reflectance factor $R_{diffuse}(\lambda)$ in the terminology of the four-flux model. The spectrophotometer also allows two transmittance modes: (1) the total transmittance mode, allowing to measure the total transmittance factor $T_{tot}(\lambda)$ in the terminology of the four-flux model; (2) the direct transmittance mode, allowing to measure the collimated-to-collimated transmittance factor $T_{cc}(\lambda)$ in the terminology of the four-flux model; the measurement geometry for this mode is CIE 0°:0°. The illumination aperture was 17 mm in diameter while the measuring aperture was 6 mm in diameter. The ratio between the illumination aperture and the measuring aperture was maximized in order to limit the edge-loss phenomenon, well-known to alter the measurement of highly translucent samples [45,46]. A built-in UV filter was used to prevent the UV-to-visible fluorescence of the sample since fluorescence is not accounted for in the investigated optical models. However, some fluorescence effect still remains, due to excitation of the optical brighteners by the short visible wavelength around 400–410 nm. Therefore, for each sample, four spectral measurements were performed: spectral reflectance factor under CIE di:8°; spectral reflectance factor under CIE de:8°), total spectral transmittance factor under CIE di:0°, and directional spectral transmittance factor under CIE 0°:0°. All measurements were performed in a completely dark room in order to prevent stray light.

2.3. Prediction algorithms

Predictions methods were applied to predict the reflectance factor of a sample with a different thickness. Analytical models rely on a set of assumptions on the material's optical properties, such as absorption and scattering parameters and the way light propagates through a layer of a given thickness. These models predict the spectral reflectance and transmittance factors of the layer, accounting for the interfaces with the bordering media (*e.g.* air, background). On the other hand, numerical approaches use known spectral reflectance factors or color coordinates of training samples with certain thicknesses, and apply regression methods in order to predict the spectral reflectance or the color coordinates of samples with other thicknesses.

2.3.1. Optical analytical models

In this comparative study, 2 two-flux models and 2 four-flux models recently investigated [40,47] were used. The first two-flux model investigated was the Kubelka–Munk model associated with the Saunderson correction [48]. This model relies on analytical formulas allowing to derive the material's optical parameters from the calibration sample (inverse model). The model predicts the spectral reflectance and transmittance factors of layers of known thicknesses as functions of the model's optical parameters (direct model). This model is denoted **2F-RT** hereinafter. The second two-flux model investigated, denoted **dir2F-RT** hereinafter, is similar to the **2F-RT** model, except that it considers light to be mainly directional within samples. This assumption has proved to be more accurate for reflectance factor predictions of thin samples of dental materials (between hundreds of microns to a few mm) [49]. The internal reflectance of the air–material interface used in the Saunderson correction is 4% in the **dir2F-RT** model whereas it is 60% in the **2F-RT** model. The implementation of these models and discussion about their physical assumptions and plausibility are given in literature [25].

The four-flux models considered in this study are extensions of the model proposed by Maheu et al. [39]. They consider separately the propagation and mutual exchanges of two diffuse and two directional light fluxes and predict a specular reflectance, a diffuse reflectance, a direct transmittance and a diffuse transmittance for any sample. The first four-flux model tested is described by Eymard et al. [40], and is denoted **Eymard4F-RT** hereinafter. The implementation of this model is detailed in literature [25,40]. The second model, denoted as **RTE-4F-RT**, is similar to the first one but with a refined calculation of the internal reflectance of the upper and lower interfaces of the material layer, using look-up tables calculated using the Radiative Transfer Equation [50,51] for translucent materials [47].

2.3.2. Numerical models

In contrast with optical models, for which the optical measurement of one calibration sample suffices, numerical models need a certain number of samples of different thicknesses to be trained. The number of training samples determines the prediction accuracy of the spectral reflectance factor of samples with other thicknesses. As the number of samples available in this study was limited, available samples were divided into training and test sets following a leaving one out cross-validation approach (CV-LOO). This was carried out for each material and shade, therefore, for a given material, the number n of samples available is divided into n-1 samples in the training set, and 1 sample in the test set. The sample in the test set can be any of the n samples, and each of them has been considered in turn. This means that all samples will be part of the training and test sets at some point, but will never belong to both at the same time.

With this type of predictive models, it is interesting to observe the prediction accuracy according to whether the thickness of the sample tested is within or beyond the range of thicknesses of the samples in the training set (which corresponds to interpolation and extrapolation approaches, respectively).

For the present study, two numerical models were investigated. The first one, denoted **PCA-PCHIP**, was previously described in literature [26] and it is based on a Principal Components Analysis approach [52]. It allows to use the spectral reflectance factors of the training set to predict the spectral reflectance factors of new samples. In this model, the spectral reflectance factors corresponding to the training set are converted into a set of Principal Components (a_i) and weighting coefficients α_i. These principal components are linear combinations of the original wavelengths that capture the maximum variance in the data. Then, a subset of the principal components, that capture a significant portion of the total variance, is selected, and regression predictive techniques are applied to predict the weighting coefficients that would correspond to new reflectance factors. The reflectance factor of the test sample can be estimated by multiplying those predicted coefficients with their corresponding singular vectors, as shown in Eq. (1).

$$R(\lambda) = \alpha_1 a_1(\lambda) + \alpha_2 a_2(\lambda) + \cdots + \alpha_n a_n(\lambda) \quad (1)$$

Choosing an appropriate number of principal components is important in order to develop models that are both accurate and efficient to predict unseen data. Previous studies have shown that for similar [26] and even more complex [53] type of data sets, optimal performance can be obtained when using 3 principal components.

The second numerical model, denoted **L*a*b*-PCHIP**, previously described in the literature [41], directly provides color estimations. This model follows a similar approach to the previous one, but uses CIE-L*a*b* values as the input data for the regression models instead of reflectance factors. Since each CIE-L*, CIE-a* and CIE-b* coordinates were predicted individually, three different models were computed for each test sample.

For both numerical methods, Piecewise Cubic Hermite Interpolating Polynomial (PCHIP) [54] was used as fitting regression method for obtaining the weighting coefficients and color coordinates, respectively. PCHIP is a mathematical approach used in numerical analysis to interpolate data points. It is a type of spline interpolation method whose goal is to create a smooth curve passing through a given set of data points. This regression method has the advantage of preserving monotonicity, and therefore, this property makes PCHIP particularly useful when interpolating data that represents monotonic trends, which is the case of our data.

2.4. Performance metrics

The measured or predicted spectral reflectances were converted into CIE1976 L*a*b* coordinates, by selecting a D65 illuminant and a perfect white diffuser under this illuminant as white reference for chromatic adaptation. As per the current recommendation by the International Commission on Illumination (CIE) [20], the total color differences between CIE-L*a*b* values corresponding to the measured and predicted data were calculated using the CIEDE2000(1:1:1) total color difference formula (Eq. (2)):

$$\Delta E_{00} = \left[\left(\frac{\Delta L'}{K_L S_L} \right)^2 + \left(\frac{\Delta C'}{K_C S_C} \right)^2 + \left(\frac{\Delta H'}{K_H S_H} \right)^2 + R_T \left(\frac{\Delta C'}{K_C S_C} \right) \left(\frac{\Delta H'}{K_H S_H} \right) \right]^{\frac{1}{2}} \quad (2)$$

This was proven to fit better with human perception for dental specific shade matching tasks [55]. ΔE_{00} values were assessed based on the specific perceptibility threshold (PT) $\Delta E_{00} = 0.8$ and acceptability threshold (AT) $\Delta E_{00} = 1.8$ for dentistry, as reported in literature [56,57] and recommended by the ISO/TR 28642:2016 [58].

Table 2
Statistics of error metrics between measured and predicted reflectance factors for the different optical models (78 specimens considered for prediction).

	2F-RT	dir2F-RT	Eymard4F-RT	RTE-4F-RT
Mean ΔE_{00}	5.35	2.49	1.24	0.72
95th percentile	17.96	4.81	2.89	1.82
<AT%	30.77	38.46	80.77	94.87
<PT%	7.69	3.85	35.90	65.38

3. Results

Fig. 1 shows all ΔE_{00} values between predicted and measured colors for all materials and shades and all six predictive models evaluated.

For the optical models, Table 2 shows the mean ΔE_{00}, the 95th percentile and the percentage of samples below AT_{00} and PT_{00} values for all the unknown data, i.e., all materials and all thicknesses excluding the calibration sample (1.2 mm). All optical models yield a color difference of 0 for the calibration sample, since the calibration of these models involves employing reversible protocols in order to identify the optical parameters that minimize color difference for the calibration sample.

The prediction accuracy of the 2F-RT model deviates quickly as the thickness deviates from the calibration thickness, while it is more stable for the more advanced RTE-4F-RT model which indicates that the latter better describes the light propagation in the evaluated samples. For the same reasons, the 2F-RT and dir2F-RT models are rather inaccurate, while the Eymard4F-RT model achieved an average ΔE_{00} color difference of 1.24 below AT_{00}. The best performance among the optical models was obtained for the RTE-4F-RT model, which achieved an average ΔE_{00} color difference of 0.72, slightly below PT_{00}, while the 95th percentile is at 1.82, slightly above AT_{00}, for the 78 evaluated samples.

For the numerical models, more than one sample are needed to train the algorithms, and therefore a CV-LOO approach was used to fully exploit the available data. For these models, it is important to consider that in the given experimental context, different modeling behaviors may arise when estimating the data (spectral reflectance factor or color values) of samples with thicknesses beyond the range covered by the training data (extrapolation) compared to thickness within the training data range (interpolation). Therefore, it is worth examining whether the prediction performance changes by excluding extreme values and focusing solely on values falling within the range of available data (intermediate values well-represented in the training set).

Tables 3 and 4 show the mean ΔE_{00}, the 95th percentile and the percentage of samples below AT_{00} and PT_{00} values for all materials when employing the interpolation and extrapolation approach or interpolation only approach, respectively.

As expected, better performance was achieved when following an interpolation approach, with average color differences around ΔE_{00} =

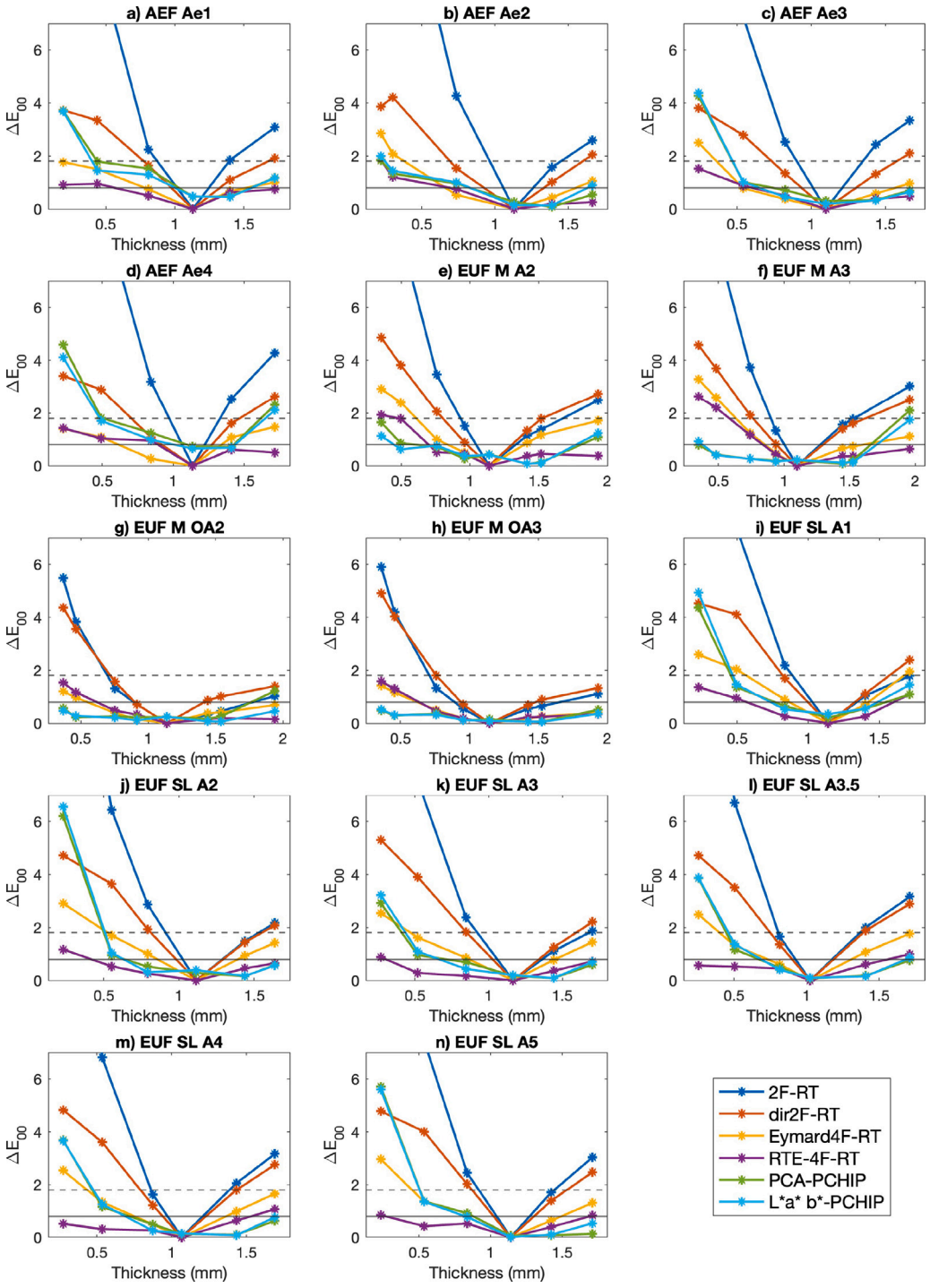

Fig. 1. ΔE_{00} values between measured and predicted data, and corresponding PT_{00} (solid) and AT_{00} (dotted) lines, for all materials (a–d: Aura Easy Flow, e–h: Estelite Universal Flow Medium, i–m: Estelite Universal Flow SuperLow) and each predictive model evaluated.

Table 3
Statistics of error metrics between measured and predicted values for the different numerical models (interpolation and extrapolation approach — 92 specimens considered for prediction).

	PCA-PCHIP	L*a*b*-PCHIP
Mean ΔE_{00}	0.99	0.97
95th percentile	4.23	4.09
<AT%	85.87	88.04
<PT%	65.22	65.22

Table 4
Statistics of error metrics between measured and predicted values for the different numerical models (interpolation only approach — 64 specimens considered for prediction).

	PCA-PCHIP	L*a*b*-PCHIP
Mean ΔE_{00}	0.51	0.48
95th percentile	1.41	1.44
<AT%	98.44	100.00
<PT%	76.56	79.69

0.5, versus those obtained for an approach including both interpolation and extrapolation, whose average color differences obtained were almost twice as large, around $\Delta E_{00} = 1.0$. For this type of models, whose performance relies on regression methods, it is extremely important to work with data within a known domain, which would be the case of interpolation, but not of extrapolation. However, even for the case were extrapolated spectra are considered, very good results were obtained, since similar performances were obtained with the four-flux optical models ($< AT\%$ above 85% and $< PT\%$ above 65%), and even much better than the more simple two-flux optical models.

4. Discussion

In restorative dentistry, achieving a natural and seamless blend with the surrounding teeth is essential. Dentists must accurately match the color and shade of the restorative materials with the patient's existing teeth to achieve a harmonious and natural look. In this regard, spectral reflectance is paramount for material characterization and, therefore, being able to properly predict it can have significant applications in the dental field.

This research paper presents a comprehensive investigation into the performance of optical models including 2F-RT, dir2F-RT, Eymard4F-RT, and RTE-4F-RT and numerical models, specifically PCA-Based and L*a*b*-Based models, for predicting color of various dental materials. It delves into the pros and cons of these models, considering factors such as accuracy, ease of implementation, sample requirements, and adaptability to different scenarios.

From the values presented in Fig. 1, we can see that for all of the models a U-shaped trend is observed for the CIEDE2000 color differences as a function of the sample thickness. For the optical models, the predictions according to the thickness rely necessarily on an extrapolation approach since only one sample is used for calibration. An ideal model should provide accurate predictions regardless of the thickness of the calibration sample and the test thicknesses evaluation. In practice however, due to the approximations made by the model in terms of light propagation, better predictions are obtained when the thickness of the test sample is close to the one of the calibration. In this regard, for the numerical models it is logical to expect better results for samples centered within the data range used.

In the case of optical models, the prediction accuracy of two-flux models is limited due to the rather high translucency of dental materials while their physical assumptions are satisfied with highly scattering materials only [25]. The translucency of dental materials is better managed by the four-flux models, especially by the RTE-4T-RT, for which the internal reflections at the bordering interfaces are more finely quantified thanks to computations based on a Radiative Transfer model [47]. This is why the latter model enables reflectance factor predictions with color differences below the acceptability threshold for most materials evaluated, and in many cases even below the perceptibly threshold.

Also, it is important to consider that optical models rely on physical descriptions of light matter interaction to link macroscopic measurements, namely reflectance and transmittance factors of a layer, to its optical parameters. As such, optical models tend to be more sensible than numerical approaches to measurements inaccuracies. One source of deviation known in the field of translucent material [45] is edge-loss phenomenon, which occurs when light exits the materials layer by its boundary and thus, does not reach the sensor in both reflectance and transmittance measurements [46]. In the case of dental materials, this phenomenon affects longer wavelengths (red light) more than shorter wavelengths (blue light), since longer wavelengths usually propagate further into these materials. This phenomenon is not accounted for in optical models and might be falsely interpreted as absorption and/or scattering. Edge-loss also occurs with numerical models but it is included in the training data, since edge-loss may vary with respect to the sample thickness, however it can be a limit to the accuracy of numerical models too.

Regarding the numerical models, it should be noted that for the extrapolation cases, generally worse results were obtained. This reflects the importance of predicting data that is within the range of data used to train the models, or in the worse case scenario, when an extrapolation approach has to be used, it is important to keep in mind the limits of the models and know that the farther we move away from the range of data, the worse the results obtained will be, as clearly show the results presented in Tables 4 and 3.

In comparing optical and numerical models, it becomes evident that each approach has its own set of advantages and drawbacks. On one hand, optical models aim to surpass numerical approaches by understanding the intricate interactions between light and materials. These models enable spectral material characterization which can be useful for material manufacturers, requiring only one sample for calibration and allowing adaptation for predicting reflectance or transmittance factors. They can also be adapted for different contexts, for directional or diffuse lighting, with or without background, etc. However, these models demand more measurements and adapted instrumentation, for example, four-flux models need an optical bench with integrating sphere allowing reflectance measurement (specular component included and excluded) and transmittance measurements (diffuse and direct), which are considerably more complex than those needed for numerical models, also since four-flux model rely on an optimization algorithm for their calibration, the calibration step requires a longer calculation time (about 5 s for the Eymard4F-RT model, and about 2 min for the RTE-4F-RT model on a standard computer). The longer computation time makes them less straightforward than numerical models and less suitable for integration into handheld devices.

On the other hand, numerical models are quick to run and easy to implement. They are also more suitable for integration into handheld devices since they only rely on reflectance factor measurements. Moreover, they can be enhanced with other algorithm types, providing flexibility in optimization. However, limitations include material dependency, the necessity for multiple samples to train the models, and reduced accuracy in extrapolation scenarios. Despite these drawbacks, numerical models remain more accurate than many optical models for extrapolation. Also, it is important to take into account that for the L*a*b*-PCHIP model, reflectance estimation is not possible, since it only works with color data. Indeed, although the main purpose of all approaches is to predict color, spectral approaches (analytical or numerical) are more reliable since they enable to predict the color under any illuminant, not only the device's light source, and are less subject to metamerism. The L*a*b*-PCHIP model, working with color measurements can be a drawback if the goal is to characterize the materials, however, it can be also an advantage for clinical scenarios, where color data is easier to acquire than spectral data.

It is also worth highlighting that, both numerical and optical approaches can be adapted to the case of multilayered materials. The accuracy of two-flux models for predicting the reflectance factor of bilayered samples has been demonstrated without the need for additional calibration compared to single layer materials [59]. Four-flux models for layered materials have been also previously used [60,61], but their accuracy applied to dental materials remains to be tested. Numerical models calibrated using multilayered training samples of dental materials have also been proposed [41,53], showing good prediction accuracy, and new methods relying solely on single layer samples are under development. Therefore, based on the results of this study, the research hypothesis is accepted, since optical and numerical models can provide similar prediction accuracy, although, this is only true for the four-flux optical models, as there are significant differences in performance for the two-flux models.

The comparison between optical and numerical approaches, along with practical considerations, is summarized in Table 5.

Table 5
Summary of pros and cons of optical and numerical approaches.

Approach	Optical (Extrapolation)	Numerical (Interpolation)
Average color difference	Two-flux: > AT_{00} RTE-4F-RT: < PT_{00}	interpolation and extrapolation: < AT_{00} interpolation: < PT_{00}
Instrument required	d:8°	d:8° or 45°:0°
Calibration samples required	1	N
Prediction enabled	Reflectance/Transmittance	Reflectance
Applicable to layered materials	Yes	Yes
Calculation time	Two-flux: $\sim 10^{-3}$ s Four-flux: ~10 s	$\sim 10^{-3}$ s

Bearing the limitations in mind, it has become clear that both types of models, optical and numerical, have great potential to be a valuable aid in the dental industry. Numerical models are well-suited for scenarios where accuracy, speed, and ease of implementation are critical, especially for handheld devices. Optical models, meanwhile, despite their intricacies, are valuable for material characterization especially during their formulation, but maybe less practical for embedded systems due to their computational demands. Future work should include a wider range of dental materials, as for example ceramics. Nevertheless, the high accuracy obtained with the shades and materials already tested, confirms that the proposed methods for reconstructing reflectance factor and color can already be used.

5. Conclusions

This research highlights the importance of choosing the appropriate model based on the specific requirements of the application. Optical and numerical models can provide similar prediction accuracy, therefore the choice of model for color prediction of dental materials can be based on the user's needs or available resources without compromising its outcome.

The findings presented in this paper contribute to a better understanding of the strengths and limitations of numerical and optical models, facilitating informed decision-making in the selection of prediction methods.

References

[1] Lee YK. Translucency of human teeth and dental restorative materials and its clinical relevance. J Biomed Opt 2015;20(4):045002.

[2] Johnston WM. Review of translucency determinations and applications to dent mater. J Esthet Restor Dent 2014;26(4):217–23. http://dx.doi.org/10.1111/jerd.12112.

[3] Arif R, Yilmaz B, Johnston WM. In vitro color stainability and relative translucency of CAD-cam restorative materials used for laminate veneers and complete crowns. J Prosthet Dent 2019;122(2):160–6. http://dx.doi.org/10.1016/j.prosdent.2018.09.011.

[4] Ruiz-López J, Espinar C, Lucena C, de la Cruz Cardona J, Pulgar R, Pérez MM. Effect of thickness on color and translucency of a multi-color polymer-infiltrated ceramic-network material. J Esthet Restor Dent 2022. http://dx.doi.org/10.1111/jerd.12952.

[5] Jouhar R, Ahmed MA, Khurshid Z. An overview of shade selection in clinical dentistry. Appl Sci 2022;12(14):6841.

[6] Pop-Ciutrila I-S, Ghinea R, Colosi HA, Ruiz-López J, Perez MM, Paravina RD, et al. Color compatibility between dental structures and three different types of ceramic systems. BMC Oral Health 2021;21:1–10.

[7] Todorov R, Peev T, Zlatev S, et al. Shade guides used in the dental practice. J IMAB–Annual Proc Sci Papers 2020;26(2):3168–73.

[8] Alnusayri MO, Sghaireen MG, Mathew M, Alzarea B, Bandela V, Sghaireen MG. Shade selection in esthetic dentistry: A review. Cureus 2022;14(3).

[9] Ruiz-López J, Perez MM, Lucena C, Pulgar R, López-Toruño A, Tejada-Casado M, et al. Visual and instrumental coverage error of two dental shade guides: an in vivo study. Clinical Oral Investigat 2022;26(9):5961–8.

[10] Hein S, Modrić D, Westland S, Tomeček M. Objective shade matching, communication, and reproduction by combining dental photography and numeric shade quantification. J Esthetic Restorative Dentistry 2021;33(1):107–17.

[11] Akl MA, Sim CPC, Nunn ME, Zeng LL, Hamza TA, Wee AG. Validation of two clinical color measuring instruments for use in dental research. J Dentistry 2022;125:104223.

[12] Akl MA, Mansour DE, Zheng F. The role of intraoral scanners in the shade matching process: a systematic review. J Prosthodontics 2023;32(3):196–203.

[13] Beneducci WP, Teixeira ML, Pedrini H. Dental shade matching assisted by computer vision techniques. Comput Methods Biomech Biomed Eng Imag Visualiz 2023;11(4):1378–96.

[14] Moussa R. Dental shade matching: Recent technologies and future smart applications. J Dent Health Oral Res 2021;2:1–10.

[15] Ebeid K, Sabet A, Omar E, Della Bona A. Accuracy and repeatability of different intraoral instruments on shade determination compared to visual shade selection. J Esthetic Restorative Dentistry 2022;34(6):988–93.

[16] Soufdoost RS, Emam F, Lari HA, Ghomi AG, Alihemmati M. Evaluation of accuracy of conventional visual, spectrophotometric and 3D scanning methods by using two shade guide systems. Sci Arch Dental Sci 2019;2(12).

[17] Jain M, Jain V, Yadav NR, Jain S, Singh S, Raghav P, et al. Dental students' tooth shade selection ability in relation to years of dental education. J Family Med Primary Care 2019;8(12):4010.

[18] Śmielecka M, Dorocka-Bobkowska B. Effects of different light sources on tooth shade selection.. Dental Med Problems 2020;57(1):61–6.

[19] Neppala G, Rajaraman V, Ashok V, Maiti S, et al. Effect of aging of shade guide and its influence on shade selection-an in vitro study. J Coastal Life Med 2022;10:226–36.

[20] Fairchild MD. CIE 015:2018 colorimetry, 4th edition. The international commission on illumination, Vienna, Austria. Color Res Appl 2019;44(4):674–5.

[21] Espinar C, Della Bona A, Tejada-Casado M, Pulgar R, Pérez MM. Optical behavior of 3D-printed dental restorative resins: Influence of thickness and printing angle. Dent Mater 2023.

[22] Kim H-K, Kim S-H, Lee J-B, Han J-S, Yeo I-S, Ha S-R. Effect of the amount of thickness reduction on color and translucency of dental monolithic zirconia ceramics. J Adv Prosthodontics 2016;8(1):37–42.

[23] Pop-Ciutrila IS, Ghinea R, Dudea D, Ruiz-López J, Pérez MM, Colosi H. The effects of thickness and shade on translucency parameters of contemporary, esthetic dental ceramics. J Esthetic Restorative Dentistry 2021;33(5):795–806.

[24] Hébert M, Hersch RD. Review of spectral reflectance models for halftone prints: Principles, calibration, and prediction accuracy. Color Res Appl 2014;40(4):383–97. http://dx.doi.org/10.1002/col.21907.

[25] Duveiller V, Clerc R, Eymard J, Salomon J-P, Hébert M. Performance of two-flux and four-flux models for predicting the spectral reflectance and transmittance factors of flowable dental resin composites. Dent Mater 2023;39(8):743–55.

[26] Tejada-Casado M, Ghinea R, Perez MM, Lübbe H, Pop-Ciutrila I, Ruiz-López J, Herrera L. Reflectance and color prediction of dental material monolithic samples with varying thickness. Dent Mater 2022;38(4):622–31. http://dx.doi.org/10.1016/j.dental.2021.12.140.

[27] Kubelka P, Munk F. Ein beitrag zur optik der farbanstriche. Z Technische Phys 1931;11a:593–601.

[28] Kubelka P. New contributions to the optics of intensely light-scattering materials. Part I. J Opt Soc Am 1948;1138(5):448–57. http://dx.doi.org/10.1364/JOSA.38.000448.

[29] Kubelka P. New contributions to the optics of intensely light-scattering materials. Part II: Nonhomogeneous layers. J Opt Soc Am 1954;44(4):330–5. http://dx.doi.org/10.1364/JOSA.44.000330.

[30] Spitzer D, Ten Bosch J. The absorption and scattering of light in bovine and human dental enamel. Calcif Tissue Res 1975;60:129–37. http://dx.doi.org/10.1007/BF02547285.

[31] Miyagawa Y, Powers J, O'Brien W. Optical properties of direct restorative materials. J Dent Res 1981;60:890–4. http://dx.doi.org/10.1177/00220345810600050601.

[32] Ragain J, Johnston W. Accuracy of kubelka-munk reflectance theory applied to human dentin and enamel. J Dent Res 2001;80:449–52. http://dx.doi.org/10.1177/00220345010800020901.

[33] Pop Ciutrila IS, Ghinea R, Gomez MMP, Colosi HA, Dudea D, Badea M. Dentine scattering, absorption, transmittance and light reflectivity in human incisors, canines and molars. J Dent 2015;43(9):1116–24. http://dx.doi.org/10.1016/j.jdent.2015.06.011.

[34] Yoshimura H, Chimanski A, P.F. C. Systematic approach to preparing ceramic-glass composites with high translucency for dental restorations. Dent Mater 2015;31:1188–97. http://dx.doi.org/10.1016/j.dental.2015.06.015.

[35] Schabbach L, dos Santos B, De Bortoli L, Fredel M, B. H. Application of Kubelka-Munk model on the optical characterization of translucent dental zirconia. Mater Chem Phys 2021;258:123994. http://dx.doi.org/10.1016/j.matchemphys.2020.123994.

[36] Sarah SM, Shereen SA, Johnston WM. Accuracy of kubelka–munk reflectance theory for dental resin composite material. Dent Mater 2012;28(7):729–35. http://dx.doi.org/10.1016/j.dental.2012.03.006.

[37] Kristiansen J, Sakai M, Da Silva JD, Gil M, Ishikawa-Nagai S. Assessment of a prototype computer colour matching system to reproduce natural tooth colour on ceramic restorations. J Dent 2011;39:e45–51. http://dx.doi.org/10.1016/j.jdent.2011.11.009.

[38] Wang J, Lin J, Gil M, Seliger A, Da Silva J, Ishikawa-Nagai S. Assessing the accuracy of computer color matching with a new dental porcelain shade system. J Prostht Dent 2014;11:247–53. http://dx.doi.org/10.1016/j.prosdent.2013.07.008.

[39] Maheu B, Letoulouzan J, Gouesbet G. Four-flux models to solve the scattering transfer equation in terms of lorenz-mie parameters. Appl Opt 1984;23(19):3353–62. http://dx.doi.org/10.1364/AO.23.003353.

[40] Eymard J, Clerc R, Duveiller V, Commault B, Hebert M. Characterization of UV–Vis–NIR optical constants of encapsulant for accurate determination of absorption and backscattering losses in photovoltaics modules. Sol Energy Mater Sol Cells 2022;240:111717. http://dx.doi.org/10.1016/j.solmat.2022.111717.

[41] Tejada-Casado M, Ghinea R, Pérez MM, Ruiz-López J, Lübbe H, Herrera LJ. Development of thickness-dependent predictive methods for the estimation of the CIEL* a* b* color coordinates of monolithic and layered dental resin composites. Materials 2023;16(2):761.

[42] Ilie N, Hickel R. Resin composite restorative materials. Aust Dent J 2011;56(s1):59–66. http://dx.doi.org/10.1111/j.1834-7819.2010.01296.x.

[43] Goodacre CJ, Eugene Roberts W, Munoz CA. Noncarious cervical lesions: Morphology and progression, prevalence, etiology, pathophysiology, and clinical guidelines for restoration. J Prosthodontics 2023;32(2):e1–e18. http://dx.doi.org/10.1111/jopr.13585.

[44] ISO/TR 4049:2009. Technical Report(E): Dentistry – Polymer-based Restorative Materials, International Organization for Standardization.; 2009.

[45] Johnston W, Hesse N, Davis B, Seghi R. Analysis of edge-losses in reflectance measurements of pigmented maxillofacial elastomer. J Dental Res 1996;75(2):752–60. http://dx.doi.org/10.1177/00220345960750020401.

[46] Gevaux L, Simonot L, Clerc R, Gerardin M, Hebert M. Evaluating edge loss in the reflectance measurement of translucent materials. Appl Opt 2020;59(28):8939–50. http://dx.doi.org/10.1364/AO.403694.

[47] Gautheron A, Clerc R, Duveiller V, Simonot L, Montcel B, Hébert M. On the validity of two-flux and four-flux models for light scattering in translucent layers: angular distribution of internally reflected light at the interfaces. Opt Express 2024;32:6. http://dx.doi.org/10.1364/OE.510888.

[48] Saunderson J. Calculation of the color of pigmented plastics. JOSA 1942;32:727–36.

[49] Duveiller V, Gevaux L, Clerc R, Salomon J-P, Hebert M. Reflectance and transmittance of flowable dental resin composite predicted by the two-flux model: on the importance of analyzing the effective measurement geometry. In: Color imag conf. 2020, (28):Society for Imaging Science and Technology; 2020, p. 313–20. http://dx.doi.org/10.2352/issn.2169-2629.2020.28.50.

[50] Chandrasekhar S. Radiative transfer. In: Dover books on physics. New york: Dover publications inc.; 1960.

[51] Ishimaru A. Wave propagation and scattering in random media, vol. 2, New york: Academic press; 1988, p. 336–93.

[52] Jolliffe IT, Cadima J. Principal component analysis: a review and recent developments. Philos T R Soc A 2016;374(2065):20150202. http://dx.doi.org/10.1098/rsta.2015.0202.

[53] Tejada-Casado M, Ghinea R, Pérez M, Cardona J, Ionescu A, Lübbe H, et al. Color prediction of layered dental resin composites with varying thickness. Dent Mater 2022;38(8):1261–70. http://dx.doi.org/10.1016/j.dental.2022.06.004.

[54] Catmull EE, Rom R. A class of local interpolating splines. Comput Aided Geom Design 1974;317–26. http://dx.doi.org/10.1016/B978-0-12-079050-0.50020-5.

[55] Pecho OE, Ghinea R, Alessandretti R, Pérez MM, Della Bona A. Visual and instrumental shade matching using CIELAB and CIEDE2000 color difference formulas. Dent Mat 2016;32(1):82–92. http://dx.doi.org/10.1016/j.dental.2015.10.015.

[56] Paravina RD, Ghinea R, Herrera LJ, Bona AD, Igiel C, Linninger M, et al. Color difference thresholds in dentistry. J Esthet Restor Dent 2015;27:S1–9. http://dx.doi.org/10.1111/jerd.12149.

[57] Paravina RD, Pérez MM, Ghinea R. Acceptability and perceptibility thresholds in dentistry: a comprehensive review of clinical and research applications. J Esthet Restor Dent 2019;31(2):103–12. http://dx.doi.org/10.1111/jerd.12465.

[58] ISO/TR 28642:2016. Technical report(e): dentistry - guidance on color measurements, Geneva: International Organization for Standardization.; 2016.

[59] Duveiller V, Kim E, Locquet M, Gautheron A, Clerc R, Salomon J, et al. Predictions of the reflectance factor of translucent layered dental resin composites using two-flux models: assessing the importance of the interface reflectance parameter. In: Color and visual computing symposium 2022, vol. 3271. CEUR Workshop; 2022.

[60] Rozé C, Girasole T, Tafforin A-G. Multilayer four-flux model of scattering, emitting and absorbing media. Atmos Environ 2001;35(30):5125–30. http://dx.doi.org/10.1016/S1352-2310(01)00328-4.

[61] Tonon C, Rozé C, Girasole T, Dinguirard M. Four-flux model for a multilayer, plane absorbing and scattering medium: application to the optical degradation of white paint in a space environment. Appl Opt 2001;40(22):3718–25. http://dx.doi.org/10.1364/AO.40.003718.